Journal of Catalysis 287 (2012) 178–189

Contents lists available at SciVerse ScienceDirect

Journal of Catalysis

journal homepage: www.elsevier.com/locate/jcat

Reproducible preparation of Au/TS-1 with high reaction rate for gas phase epoxidation of propylene

Wen-Sheng Lee [a], M. Cem Akatay [b], Eric A. Stach [b,c], Fabio H. Ribeiro [a], W. Nicholas Delgass [a,*]

[a] Forney Hall of Chemical Engineering, Purdue University, 480 Stadium Mall Drive, West Lafayette, IN 47907, USA
[b] School of Materials Engineering and Birck Nanotechnology Center, Purdue University, West Lafayette, IN 47907, USA
[c] Center for Functional Nanomaterials, Brookhaven National Laboratory, Upton, NY 11973, USA

ARTICLE INFO

Article history:
Received 15 October 2011
Revised 21 December 2011
Accepted 22 December 2011
Available online 28 January 2012

Keywords:
Propylene epoxidation
Au/TS-1
Catalyst preparation: effect of pH
Mixing time
Temperature
Gold clusters
Stability for PO reaction

ABSTRACT

A refined and reliable synthesis procedure for Au/TS-1(Si/Ti molar ratio ~100) with high reaction rate for the direct gas phase epoxidation of propylene has been developed by studying the effects of pH of the gold slurry solution, mixing time, and preparation temperature for deposition precipitation (DP) of Au on TS-1 supports. Au/TS-1 catalysts prepared at optimal DP conditions (pH ~ 7.3, mixing for 9.5 h, room temperature) showed an average PO rate ~160 $g_{PO}\ h^{-1}\ kg_{Cat}^{-1}$ at 200 °C at 1 atm. A reproducibility better than ±10% was demonstrated by nine independent samples prepared at the same conditions. These are the highest rates yet reported at 200 °C. No visible gold particles were observed by the HRTEM analysis in the fresh Au/TS-1 with gold loading up to ~0.1 wt%, indicating that the gold species were smaller than 1 nm. Additionally, the rate per gram of Au and the catalyst stability increased as the Au loading decreased, giving a maximum value of 500 $g_{PO}\ h^{-1}\ g_{Au}^{-1}$, and Si/Ti molar ratios of ~100 gave the highest rates.

© 2011 Elsevier Inc. All rights reserved.

1. Introduction

Propylene oxide (PO) is a high value-added industrial chemical for producing useful polymeric materials, such as polyurethane [1,2]. However, the major PO production routes, the chlorohydrin and hydroperoxide processes, involve multiple stages and require additional separation and/or purification units that increase the cost of PO [1,2]. Therefore, a single-step, direct catalytic partial oxidation of propylene to PO using molecular oxygen has long been desired. The discovery by Haruta and coworkers that nanoscale gold particles on titania supports provide a highly selective (~99%) route to gas phase PO production using a mixture of propylene, oxygen, and hydrogen under ambient pressure with water as the only byproduct has opened a new page in the production of PO [3,4]. Although the selectivity is up to commercial standards, the activity, as well as the catalyst stability, is not yet there. For the early catalysts, the propylene conversion reached only around 1% and the catalysts deactivated within several hours [4]. Since then, gold catalysts have been extensively studied in order to improve PO catalytic performance.

Early studies on the effect of the support suggested that higher titanium dispersion would benefit the catalyst performance [5,6], which has led to the use of either mesoporous titanosilicate ($Ti–SiO_2$) [7–11], or microporous titanosilicalite-1 (TS-1) [6,12–20] as the support. The PO rate was enhanced to ~80 $g_{PO}\ h^{-1}\ kg_{Cat}^{-1}$ at 160 °C by using Au supported on mesoporous $Ti–SiO_2$ with Ba as the promoter [9]. On the other hand, using TS-1 as the support enhanced the PO rate up to ~116 $g_{PO}\ h^{-1}\ kg_{Cat}^{-1}$ at 200 °C and improved the stability to at least 40 h, while keeping the PO selectivity as high as 80% [17]. Further improvement in PO rate was achieved by either introducing mesoporous scale defects or applying an NH_4NO_3 pretreatment to the TS-1 support before gold deposition, and the corresponding PO rates for those catalysts reached ~130 $g_{PO}\ h^{-1}\ kg_{Cat}^{-1}$ at 200 °C [12,18]. Recently, Huang et al. reported that high PO rate, ~137 $g_{PO}\ h^{-1}\ kg_{Cat}^{-1}$ at 200 °C, could also be achieved by using a solid grinding (SG) method to deposit small gold clusters (<2 nm) on TS-1 [13]. A higher PO rate, ~160 $g_{PO}\ h^{-1}\ kg_{Cat}^{-1}$, using Au/TS-1 prepared by immobilizing the biosynthesized gold nanoparticles on the TS-1 has also been reported recently [21]. However, it should be noted this high value was achieved at reaction temperature at ~300 °C [21].

Despite the significant improvement in the PO rate, reproducibility of gold catalyst performance has been found to be an issue not only for CO oxidation but also for the PO reaction, as evidenced by the wide range of reported gold atom efficiencies ($g_{PO}\ h^{-1}\ g_{Au}^{-1}$), even for catalysts using the same support [16,17,22]. The literature also shows that the performance of gold catalysts is very sensitive to the preparation conditions [23,24]. Unlike the case for CO

* Corresponding author.
E-mail address: delgass@purdue.edu (W. Nicholas Delgass).

0021-9517/$ - see front matter © 2011 Elsevier Inc. All rights reserved.
doi:10.1016/j.jcat.2011.12.019

oxidation [25,26], detailed investigation of the effects of the preparation conditions on the PO catalytic performance has not received much attention, although an effect of the pH of the gold slurry solution had been reported [1,19]. Therefore, this work has started with refining the DP preparation conditions, including the pH of the gold slurry solution, the slurry mixing time, and the preparation temperature, to maximize the PO rate by depositing highly dispersed TEM invisible gold species on TS-1. The reproducibility of the Au/TS-1 catalytic performance for catalysts prepared at the resulting optimized preparation conditions is demonstrated by nine individual samples prepared at the same conditions. Additionally, the effect of the Si/Ti molar ratio of the TS-1 on both the gold loading uptake efficiency and the PO catalytic performance was studied. Finally, for TS-1 with favored Si/Ti molar ratios of ~100 or greater, decreasing Au loading was found to promote Au catalytic efficiency and catalyst stability after 10–100 h at reaction conditions.

2. Experimental methods

2.1. TS-1 synthesis

Titanium silicalite-1 (TS-1) with different Si/Ti molar ratios was synthesized by using the method developed by Khomane et al. [27]. For a typical synthesis of TS-1, 3.5 g of polyoxyethylene 20-sorbitan monolaurate (Tween 20, Fischer Scientific, Enzyme Grade) was mixed with 56 mL deionized water (Millipore, Synergy UV Water Purification System, 18.2 MΩ cm^{-1} resistivity, hereafter denoted as D.I. water) under vigorous stirring, followed by addition of 26–28 mL of tetrapropylammonium hydroxide (TPAOH, Alfa Aesar, 40 wt%) and 66.5–70 mL of tetraethylorthosilicate (TEOS, Aldrich, 98%). The solution was then stirred for 1–2 h at room temperature. A solution containing an appropriate amount of titanium (IV) butoxide (TBOT, Alfa Aesar, <99%) dissolved in 20 mL of isopropyl alcohol (IPA, Alfa Aesar, HPLC Grade, 99.7+%) was then added while stirring. The final solution was stirred for a minimum of 1 h at 40–45 °C before being placed in a Teflon-lined autoclave (Questron Technologies) and statically heated (without agitation) in an oven (Precision Scientific) at 140–150 °C for at least 18 h under autogenous pressure. The resulting solid was separated from the growth liquid via centrifugation (4500 rpm for 30–40 min, Eppendrof Centrifuge 5804), washed once with approximately 10–15 mL D.I. water per gram of the TS-1, and dried overnight at room temperature in a vacuum oven. Once dried, the resulting white powder (approximately ~4 g in a ceramic combustion boat (CoorsTek)) was calcined (Lindberg Blue M Tube Furnace) at 550 °C for 16 h with ramping rate of 2 °C min^{-1} in a flow of air of ~150 mL min^{-1} to remove the organic template. Silicalite-1 (S-1) was also prepared in a similar method except the step of adding titanium (IV) butoxide was omitted.

2.2. Gold deposition

Gold was deposited using the DP method as outlined by Taylor et al. [17]. A typical synthesis of Au/TS-1 with different Si/Ti molar ratios was as follows: Approximately 0.2 g of hydrogen tetrachloroaurate(III) trihydrate ($HAuCl_4 \cdot 3H_2O$, Alfa Aesar, 99.99%) was dissolved in 40 mL D.I. water, followed by addition of approximately 2 g TS-1 (the nominal gold loading ~5.5 wt%). The slurry (TS-1 and gold solution) was then stirred at 900 rpm for 30 min at room temperature. The slurry solution was then neutralized by adding specific amounts of 1 N aqueous solution of sodium carbonate (J.T. Barker Chemical Co. and/or Sigma) depending on the target pH of the gold slurry solution at the end of the pH adjustment. The Na/Au molar ratio was approximately ~4–5 when the target final pH of the gold slurry solution was ~7.3–7.5 (Mettler Toledo SevenEasy pH meter with pH Electrodes: InLab®RoutinePro). The slurry was then allowed to mix for another 5 h at room temperature after adding the base. For studying the effect of mixing time at room temperature, times ranging from 2.5 to 16 h were used. For the catalysts prepared at higher temperature, the preparation procedure was similar to the method reported in the literature [1]: The gold slurry solution was prepared and mixed for 30 min at room temperature. After the base (1 N Na_2CO_3 aqueous solution) was added to the slurry, it was heated to 70 °C over a ~30 min period and further stirred at 70 °C for another 1.5 h and the end pH of the slurry was ~7.46. The catalyst slurry at 70 °C was then directly separated in the centrifuge, and washed as described below. For all catalysts, after gold deposition, the solid was removed via centrifugation (4500 rpm for 20–30 min, Eppendrof Centrige 5804) washed by suspending the catalyst in approximately 50 mL of D.I. water, and stirred for 1–2 min. Finally, the catalysts were separated via centrifugation and dried overnight under vacuum at room temperature. The catalysts were named as 0.048Au/TS-1(100), in which 0.048 represents the gold loading in weight percent (wt%) and the number in the parenthesis represents the Si/Ti molar ratio in the TS-1.

2.3. Characterization of gold on titanium silicalite-1

The bulk structure of the TS-1 was determined using X-ray diffraction (XRD) using a Scintag X2 diffractometer with Cu Kα radiation. Samples were scanned through 15–45° (2θ) with scanning rate 1.2° min^{-1}. The local environment of the titanium in the TS-1 was evaluated by diffuse reflectance ultraviolet–visible spectroscopy (DRUV–vis) using a Varian Cary 5000 outfitted with Harrick Praying Mantis optics and $BaSO_4$ as the reference. The surface areas as well as the pore volumes were measured using nitrogen adsorption isotherms (Micromeritics ASAP 2000). Samples were degassed at 250 °C for at least 8 h before N_2 adsorption. The hydrophobicity of the TS-1 was evaluated by measuring the water sorption capacity with a thermogravimetric analyzer (TGA) using a TA Instruments DSC Q600. Prior to the TGA measurements, ~0.5 g samples were suspended into ~2 mL D.I. water and the slurry was sonicated for 2–5 min followed by aging overnight for water sorption. The excess D.I. water was then decanted and the remaining solid was further dried in the ambient environment for at least 3 days. The TGA analysis was performed by heating the dried sample (approximate 20–40 mg, ground to a fine powder, but not sieved) from room temperature to 250 °C at a ramping rate 5 °C min^{-1} in a flow of He of ~100 mL min^{-1}. The particle size of the support was determined by transmission electron microscopy for at least 300 particles (TEM, FEI Tecnai F20, 200 keV), while the gold particle size was determined by high resolution TEM (HRTEM, FEI Titan, 300 keV). TEM samples were prepared by dissolving 1–5 mg catalyst in 0.5 mL ethanol and sonicating the suspension for 5 min. The solution was then dropped on 200 mesh lacey carbon-coated copper grids, and the grids were dried for 15 min at RT. The bulk metal loadings (Au and/or Ti) were determined using atomic absorption spectroscopy (AAS, Perkin–Elmer AAnalyst 300), while surface Si/Ti molar ratio was obtained by X-ray photoelectron spectroscopy (XPS) measured with a Kratos Axis Ultra DLD spectrometer using an Al Kα monochromatic X-ray radiation at 1486.6 eV and referenced to the Si 2p line at 103.4 eV [28].

2.4. Measurement of PO reaction rates

Catalytic reaction rates were determined using a 10 mm diameter Pyrex reactor housed within a furnace and using 0.15 g catalyst of 60–80 mesh size. Approximately 1–2 g quartz sand of

70–80 mesh size was used to dilute the catalyst (corresponding to volume ratio 1:1) to improve the temperature uniformity within the catalyst bed. The quartz sand was pre-calcined at 550 °C in a flow of air for 16 h to burn off any impurities. A blank experiment was performed to ensure that no side reactions were caused by the quartz sand. A type-K thermocouple was embedded in the catalyst bed to directly measure the reaction temperature. The reactant mixture consisted of 10/10/10/70 vol% of hydrogen (Praxair, 99.999%), oxygen (Praxair, 99.999%), propylene (Matheson, 99.9%), and nitrogen (Matheson, 99.999%) with a total flow of 35 mL min^{-1}, resulting in a space velocity of 14,000 mL h^{-1} g_{cat}^{-1}. The total flow rate was confirmed by measurement at the outlet of the reactor. Typical pressure drop caused by the catalyst bed was 0–0.07 atm. A reaction temperature of 200 °C was chosen for catalytic activity testing. Each catalyst was heated in the reaction mixture from room temperature to 200 °C at a ramp rate 0.5 °C min^{-1} (~5 h) followed by at least 6 h at 200 °C. The reported PO rate, PO selectivity, and H_2 selectivity in this work were the average values between the 3rd to 5th h at 200 °C. The external mass transfer was minimized by operating the reaction at high space velocity. The internal mass transfer limitation can be neglected because the estimated Thiele modulus is much smaller than 1 [29]. To avoid on-the-shelf deactivation typical of some Au catalysts, the samples were kept from light via storing in a vial wrapped with aluminum foil and the kinetic measurements were carried out within 24 h of gold catalyst synthesis.

The reactor effluent was analyzed using an Agilent 6890 gas chromatograph outfitted with an automatic sampling valve and two sample loops. Oxygenated products (PO, ethanal (Et), propanal (Pr), acetone (Ac), and acrolein (An)) were separated using a Supelcowax 10 capillary column (0.53 mm × 60 m) and analyzed via a flame ionization detector, while inorganic products were separated by a Chromosorb 102 packed column (1/8 in. × 8 ft) and analyzed by a thermal conductivity detector. The propylene conversion, PO selectivity, and H_2 selectivity were calculated directly and defined as follows:

Propylene conversion = moles of (C_3-oxygenates + 2/3ethanal + CO_2/3)/moles of propylene in the feed.
PO selectivity = moles of PO/moles of (C_3-oxygenates + 2/3ethanal + CO_2/3).
H_2 selectivity = moles of PO/moles of H_2 converted.

Carbon balances were closed to 100 ± 5%. However, use of the nitrogen as the carrier gas in order to allow detection of H_2 by TCD prevented the quantification of trace amounts of carbon dioxide. The minimum observable CO_2 signal was ~0.18 vol% in the gas stream, corresponding to ~0.62% conversion of propylene to CO_2. Thus, the PO selectivities reported are upper bounds with a potential maximum error of 10%, that is, a selectivity of 90% indicated that the actual selectivity could be between 80% and 90%.

3. Results

3.1. Characterization of titanium silicalite-1

The MFI structure of the TS-1 with different Si/Ti molar ratios was confirmed by the X-ray diffraction pattern, as shown in Fig. 1. The presence of the orthorhombic unit cell was observed by the lack of splitting of the 2θ peak at ~24.6°. Fig. 2 shows the DRUV–vis spectra of the supports. The absorption peak at around 220 nm indicates the incorporation of the titanium into MFI framework [30]. No extraframework titanium was found in any of the TS-1 samples, as evidenced by the absence of absorption peaks in the 330 nm region [30]. Table 1 summarizes the bulk as well as surface Si/Ti molar ratio, the apparent surface area provided by the BET measurement, micropore/pore volume, and the particle size of the TS-1 materials with different Si/Ti molar ratios. The similar surface and bulk Si/Ti molar ratios in the TS-1(100) and TS-1(77) indicate a homogeneous spatial Ti distribution, while the surface Si/Ti molar ratio was found to be only half of the bulk Si/Ti molar ratio for TS-1(215). The BET surface area and pore volume generally increased as the Ti loading increased, which can be explained by the expansion of the TS-1 unit cell due to the insertion of the Ti into the MFI framework, and is consistent with previous studies [30,31]. However, all the supports had an average particle size of about 280 nm, regardless of the Si/Ti molar ratio. Fig. 3 shows TEM images of selected TS-1 samples and the corresponding particle size distributions.

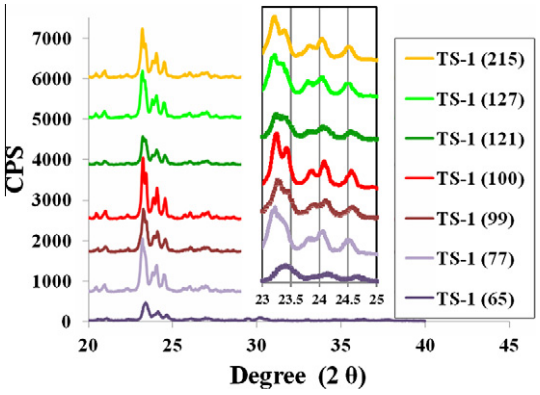

Fig. 1. XRD patterns of TS-1 supports with different Si/Ti ratios. Inset shows the lack of splitting at the 24.6° peak indicating the formation of the orthorhombic structure.

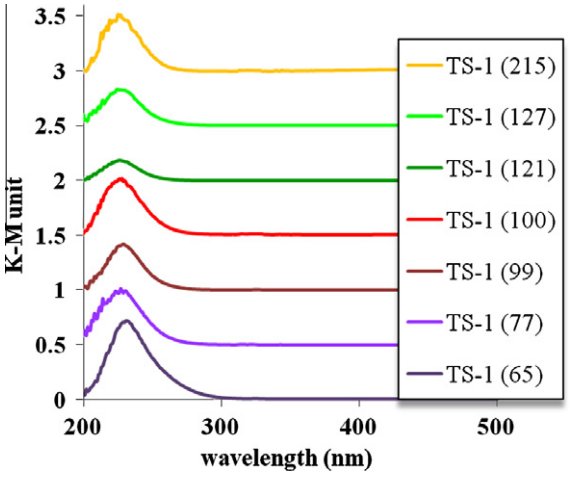

Fig. 2. UV–vis spectra of TS-1 supports with different Si/Ti ratios. The absorption at 220 nm identifies Ti with tetrahedral coordination in TS-1.

3.2. Effects of preparation conditions

In order to elucidate the effect of the preparation conditions on the gold catalysts, we first studied TS-1 with Si/Ti molar ratio = 99. A set of nine individually repeated experiments using the TS-1 with Si/Ti molar ratio = 100 was then executed to confirm the effect of the preparation conditions on the TS-1. With the mixing time (5 h) and preparation temperature (RT) kept the same, the

Table 1
Properties of TS-1 with different Si/Ti molar ratios.

Sample [a]	Surface Si/Ti molar ratio[b]	Ti content (wt%)	BET area ($m^2\ g^{-1}$)	Micropore [c] Volume ($cm^3\ g^{-1}$)	Pore volume[d] ($m^3\ g^{-1}$)	Average particle diameter[e] (nm)
S-1	ND	0	375 ± 16	0.161	0.235	ND
TS-1(215)	588	0.37	373 ± 11	0.145	0.237	ND
TS-1(121)	ND	0.65	405 ± 12	0.136	0.257	ND
TS-1(127)	ND	0.62	425 ± 11	0.146	0.257	275 ± 40
TS-1(100)	102	0.79	398 ± 15	0.143	0.243	271 ± 23
TS-1(99)	ND	0.80	406 ± 11	0.135	0.242	284 ± 26
TS-1(99)[f]	ND	0.80	403 ± 11	0.139	0.245	284 ± 26
TS-1(99)[f]	ND	0.80	386 ± 15	0.135	0.242	284 ± 26
TS-1(77)	73	1.02	418 ± 12	0.142	0.265	290 ± 34
TS-1(77)[f]	ND	1.02	415 ± 12	0.140	0.255	290 ± 34
TS-1(67)	ND	1.22	ND	ND	ND	305 ± 29

ND: not determined.
[a] The number in the parenthesis represents the bulk Si/Ti molar ratio determined by AAS.
[b] Determined by XPS analysis.
[c] Estimated by *t*-plot method.
[d] Pore volume is evaluated from the adsorption isotherm at the relative pressure about 0.97.
[e] Determined by TEM analysis.
[f] Repeat of N_2 adsorption measurement.

gold loading was found to be strongly affected by the pH of the gold slurry solution, as shown in Fig. 4a. When the pH of the gold solution increased, the gold loading decreased. Additionally, Fig. 4b shows that the gold uptake efficiency (defined as the gold loading (wt%) in the catalyst divided by the concentration of the gold precursor used for catalyst preparation) of the catalysts prepared at pH ~ 7.3 was about twice that of the catalysts prepared at pH ~ 9. As for the PO rate ($g_{PO}\ h^{-1}\ kg_{Cat}^{-1}$) of the catalysts prepared at different pHs, Fig. 5a shows an optimum pH located around ~7–8. However, if the PO rate was renormalized to represent the gold atom efficiency ($g_{PO}\ h^{-1}\ g_{Au}^{-1}$), the optimum gold atom efficiency shifted a little toward pH ~ 8, as shown in Fig. 5b. Interestingly, the samples prepared at higher pH exhibited monotonically higher H_2 selectivity, as shown in Fig. 6. Whether or not the excess Na and/or Cl, inherited from the choice of the pH of the gold slurry solution, caused an effect on the PO catalytic performance will be addressed in a subsequent paper.

Since pH of ~7–8 gave the best performance in the PO rate, the target pH was chosen as ~7.3 for studies of the slurry mixing time as well as the effect of preparation temperature. Fig. 7 shows the effect of the slurry mixing time on the gold loading and the PO rate ($g_{PO}\ h^{-1}\ kg_{Cat}^{-1}$). Increasing the slurry mixing time from 2 to 9.5 h enhanced the gold loading from ~0.056 wt% to ~0.095 wt%. The corresponding PO rate also increased from ~115 $g_{PO}\ h^{-1}\ kg_{Cat}^{-1}$ to ~160 $g_{PO}\ h^{-1}\ kg_{Cat}^{-1}$ (the average value of 9 samples shown in the Fig. 9). However, the attempt to further increase the slurry mixing time from 9.5 h to 16 h to further increase the PO rate was not successful. The gold loading was significantly increased from ~0.095 wt% to ~0.14 wt%, but the PO rate was not enhanced correspondingly but decreased slightly to ~150 $g_{PO}\ h^{-1}\ kg_{Cat}^{-1}$.

The effect of the preparation temperature on the gold loading (wt%) as well as on the PO rate ($g_{PO}\ h^{-1}\ kg_{Cat}^{-1}$) is shown in Table 2. Traditionally, higher preparation temperature (50–80 °C) has been used to shorten the preparation time required for the hydrolysis reaction to occur between the chloroauric anions and the hydroxyl anion in the gold solution [24]. Therefore, a shorter time (~2 h) was used for the sample prepared at higher temperature (~70 °C) in this study. This sample, however, did not show any benefit in the PO rate compared to the samples prepared at room temperature. The gold loading of the sample prepared at 70 °C was a little lower than that of the samples prepared at RT, but the PO rate was about half that of the samples prepared at RT, indicating that the gold atom efficiency was much worse for the sample prepared at 70 °C. Furthermore, the hydrogen selectivity of the sample prepared at 70 °C was found to be inferior to that of the samples prepared at RT.

Fig. 8 shows HRTEM images of a representative fresh catalyst, 0.1Au/TS-1(99), made by targeting the final pH of the gold slurry solution as ~7.3 for ~9.5 h mixing at room temperature. No gold particles were visible by the HRTEM analysis, indicating that only gold clusters smaller than 1 nm were present on the TS-1 after using the optimum preparation conditions proposed in this study. In order to test the reproducibility, nine individual samples prepared by the same conditions (pH ~ 7.3, mixed for ~9.5 h, room temperature) were synthesized. Fig. 9 represents the catalytic performance of the nine individual samples as a function of the reaction time. It should be noted that the PO rate of those catalysts exhibited an average value ~160 $g_{PO}\ h^{-1}\ kg_{Cat}^{-1}$ at 200 °C, and this is the highest PO rate at 200 °C yet reported and comparable to the latest reported PO rate ~160 $g_{PO}\ h^{-1}\ kg_{Cat}^{-1}$ at 300 °C by Du et al. [21]. The reproducibility of nine catalysts prepared at the optimum conditions showed that (1) the average PO rate was 158 $g_{PO}\ h^{-1}\ kg_{Cat}^{-1}$ with standard deviation 9 $g_{PO}\ h^{-1}\ kg_{Cat}^{-1}$, (2) gold atom efficiency was ~167 $g_{PO}\ h^{-1}\ g_{Au}^{-1}$ with standard deviation 22 $g_{PO}\ h^{-1}\ g_{Au}^{-1}$ (2) H_2 selectivity was 17% with standard deviation 2%. Corresponding data for (1) the selectivities to the oxygenated products (PO, ethanal (Et), propanal (Pr), acetone (Ac), and acrolein (An)) are given in Figs. S1–5, (2) the H_2 selectivity in Fig. S6, (3) the propylene conversion in Fig. S7, and (4) the production rate of the oxygenates other than PO as a function of the reaction time in Figs. S8–11.

3.3. Effects of Si/Ti molar ratio

The effect of the titanium content in the TS-1 on the gold uptake efficiency (defined as the gold loading (wt%) of the catalyst divided by the concentration of the gold precursor used in catalyst preparation) is shown in Fig. 10a and b. The gold loading was found to track the titanium loading, but the gold uptake efficiency was not a linear function of the titanium content. Moreover, the gold uptake efficiency was almost equivalent for TS-1 with Si/Ti = 215 and Si/Ti = ∞. In order to further investigate the effect of Ti content on PO catalytic performance, we prepared catalysts with different gold loadings by using either different amounts of gold precursor, different mixing times, and/or different preparation temperatures for each of the TS-1 samples with different Si/Ti molar ratios. To avoid the complexity which might be caused from the effect of the residual Na and/or Cl, all of the samples were prepared at pH ~ 7.3. Fig. 11a and b represent the PO rate ($g_{PO}\ h^{-1}\ kg_{Cat}^{-1}$) as well

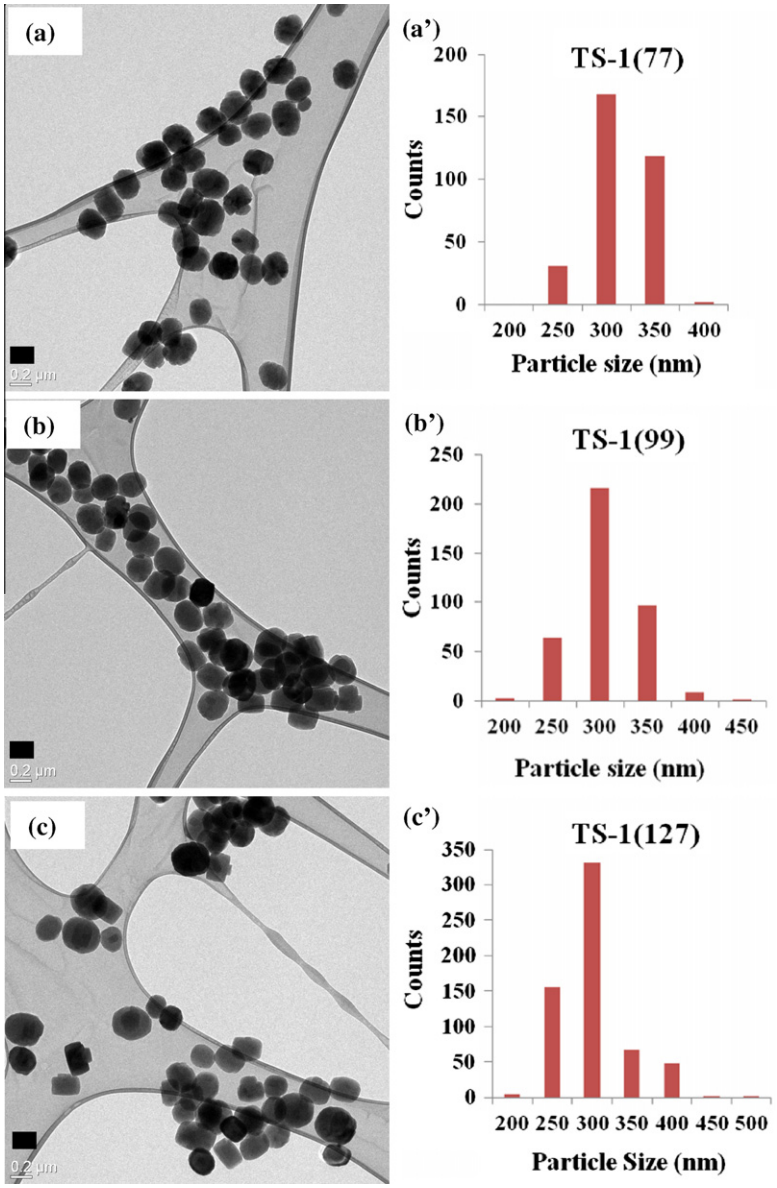

Fig. 3. TEM images of (a) TS-1(77) (b) TS-1(99) (c) TS-1(127) and the corresponding particle size distributions (a'), (b'), (c'). The scale bar represents 200 nm. The particles are shown adhering to the carbon film of the lacey carbon TEM grid.

as the gold atom efficiency ($g_{PO}\ h^{-1}\ g_{Au}^{-1}$) of the samples with different gold loadings and different Si/Ti molar ratios. For Au/TS-1 with Si/Ti of 99 or 100, the PO rate increased linearly with the gold loading up to ~0.07 wt%, which implies the number of the active sites increases as the gold loading increases in the low gold loading region (<0.07 wt%). However, the PO rate reached a plateau when the gold loading further increased up to ~0.1 wt%. For Au/TS-1(77), the PO rate was found to be able to "scale" with the gold loading over a much wider range. As the gold loading increased from ~0.03 wt% to ~0.134 wt%, the PO rate also increased from 33 $g_{PO}\ h^{-1}\ kg_{Cat}^{-1}$ to 112 $g_{PO}\ h^{-1}\ kg_{Cat}^{-1}$. Additionally, the gold atom efficiency was very sensitive to the Si/Ti molar ratio. A drastic drop of the gold atom efficiency was observed as the gold loading increased from ~0.02 wt% to ~0.1 wt% for Au/TS-1 with lower Ti content (Si/Ti ⩾99), but a less precipitous drop in the gold atom efficiency was found for Au/TS-1(77). The H_2 selectivities of the samples with different gold loadings and different Si/Ti molar ratios are shown in Fig. 12. Two categories can be classified according to the Ti content in Fig. 12. The H_2 selectivity of the Au/TS-1 with higher Ti content (Si/Ti = 77 and/or 65) was within the range of 12–20% for the gold loading from ~0.01 wt% to ~0.14 wt%. However, the H_2 selectivity of the samples with lower Ti content (Si/Ti ⩾99) was very dependent on the gold loading. A significant H_2 selectivity drop was observed from ~40% to 11.6% for Au/TS-1 (Si/Ti = 100 and/or 127) when the gold loading increased from 0.015 wt% to ~0.11 wt%. Moreover, an optimum H_2 selectivity was found for Au/TS1-1(215) when the gold loading was ~0.01 wt%.

3.4. Stability of Au/TS-1 catalysts with different PO rates

Among all of the Au–Ti catalysts studied in the literature, Au/TS-1 is one that can provide relatively good stability during catalyst operation for extended time [13,17]. Fig. 13 shows the stability performance of samples from this work with different PO rates. The samples were prepared by adjusting the gold loading via changing the concentration of the gold precursor solution, which resulted in different Au loadings and PO activities. Samples with the PO rate greater than 100 $g_{PO}\ h^{-1}\ kg_{Cat}^{-1}$ always showed decay in the PO rate

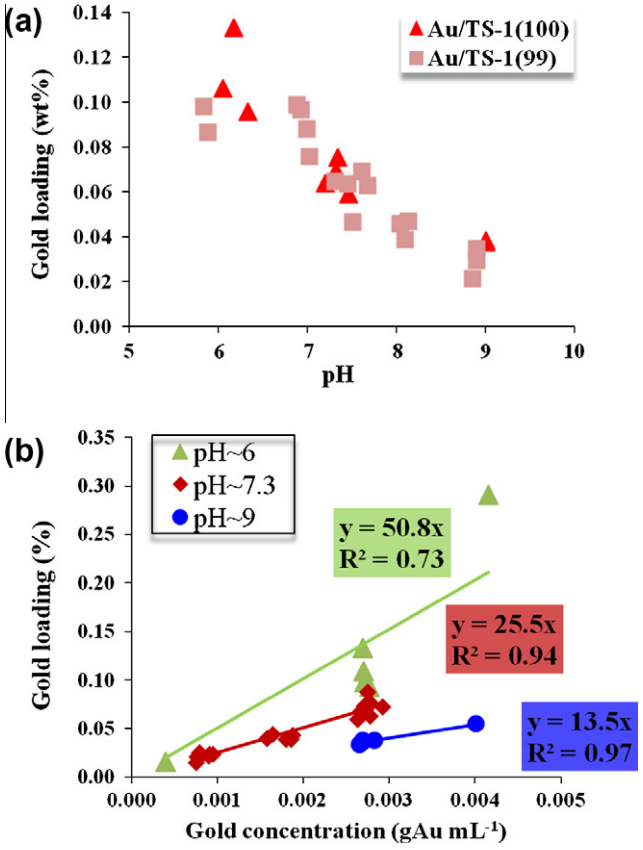

Fig. 4. (a) Gold loading of Au/TS-1(100), Au/TS-1(99) prepared at different pHs. (b) Gold loading (wt%) of Au/TS-1(99 and/or 100) as a function of the concentration of gold precursor ($HAuCl_4{\cdot}3H_2O$) used in the catalyst preparation at different pH values.

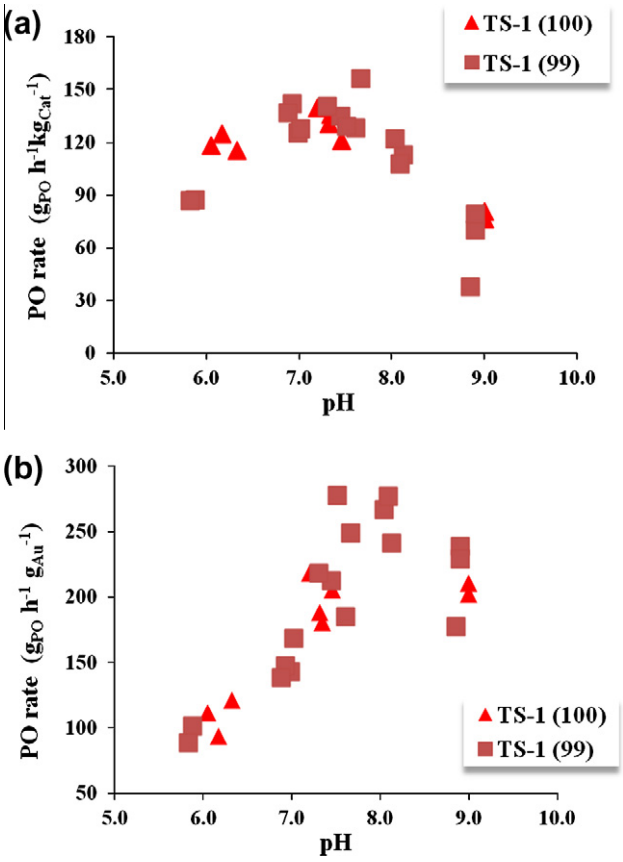

Fig. 5. (a) PO rate for Au/TS-1(100), Au/TS-1(99) prepared at different pH values. The data are reported as average values between 3rd and 5th h at 200 °C. (b) Gold atom efficiency of Au/TS-1(100), Au/TS-1(99) prepared at different pH values. The data are reported as average values between 3rd and 5th h. Reaction conditions: $H_2/C_3H_6/O_2/N_2$ = 3.5/3.5/3.5/24.5 mL min^{-1}, space velocity 14,000 mL h^{-1} g_{cat}^{-1}, reaction temperature = 200 °C.

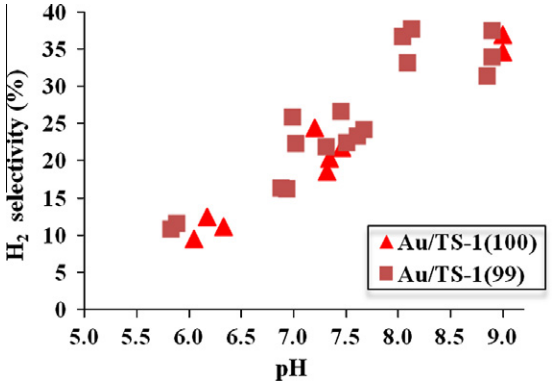

Fig. 6. H_2 selectivity of the Au/TS-1(100), Au/TS-1(99) prepared at different pH values. The data are reported as average values between 3rd and 5th h. Reaction conditions: $H_2/C_3H_6/O_2/N_2$ = 3.5/3.5/3.5/24.5 mL min^{-1}, space velocity 14,000 mL h^{-1} g_{cat}^{-1}, reaction temperature = 200 °C.

during the time they were investigated, while the stability seemed to improve as the PO rate continued to decrease. Samples with an initial PO rate of ~85 g_{PO} h^{-1} kg_{Cat}^{-1} showed very good stability over more than ~50 h, while no rate decay was observed over a periods of >100 h for a sample with a steady state PO rate of ~35 g_{PO} h^{-1} kg_{Cat}^{-1}. Furthermore, despite the similar steady state PO rate (~35–45 g_{PO} h^{-1} kg_{Cat}^{-1}) for two samples, 0.031Au/TS-1(99) and 0.023Au/TS-1(99), their kinetic behaviors within the first few hours were very different. The 0.031Au/TS-1(99), prepared by mixing the slurry for 5 h at RT with final pH ~ 5, showed higher initial PO rate which then gradually decayed to the steady state PO rate, while 0.023Au/TS-1(99), prepared at similar conditions except that the final pH was ~8.8, required a period of time to become activated and then rose to its steady state PO rate. Additionally, the HRTEM images and the corresponding gold particle size distribution analyses of two samples with very different PO rates (0.031Au/TS-1(99) with average PO rate ~45 g_{PO} h^{-1} kg_{Cat}^{-1} and 0.1Au/TS-1(99) with average PO rate ~171 g_{PO} h^{-1} kg_{Cat}^{-1}) are shown in Fig. 14. The HRTEM analysis was done after reaction at 200 °C for 3 h for both samples. The average gold particle size was found to be ~2.5 nm and ~2.9 nm for 0.031Au/TS-1(99) and 0.1Au/TS-1(99), respectively. However, it should be noted that relatively few visible gold particles were found in the 0.1Au/TS-1(99) sample.

4. Discussion

4.1. Deposition of gold

In an effort to isolate the effects of gold catalyst preparation conditions on the PO catalytic performance, the same source of TS-1 with identical chemical/physical properties should be used. Due to the fact that only small amounts of TS-1 could be obtained from each batch of TS-1 synthesis (~16 g), multiple batches of TS-1 with the same Si/Ti molar ratio were synthesized and then mixed to create the TS-1 supply for each Si/Ti ratio. Therefore, the difference observed in PO activity and/or H_2 selectivity could be unambiguously attributed to the different gold catalyst preparation conditions.

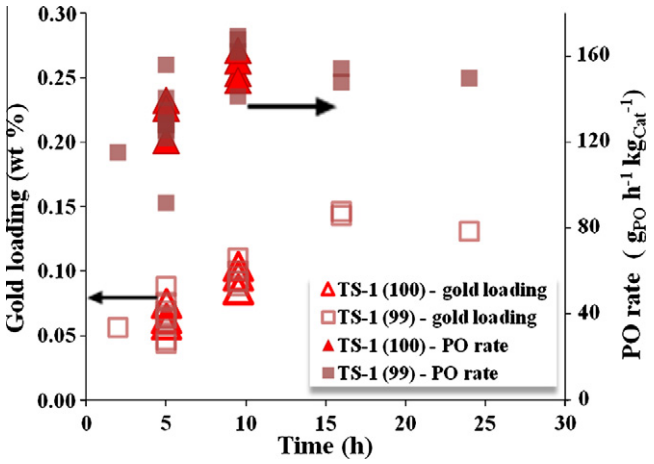

Fig. 7. Gold loading and PO rate for the Au/TS-1(100), Au/TS-1(99) prepared at different mixing times. The data are reported as average values between 3rd and 5th h. Reaction conditions: $H_2/C_3H_6/O_2/N_2$ = 3.5/3.5/3.5/24.5 mL min^{-1}, space velocity 14,000 mL h^{-1} g_{cat}^{-1}, reaction temperature = 200 °C.

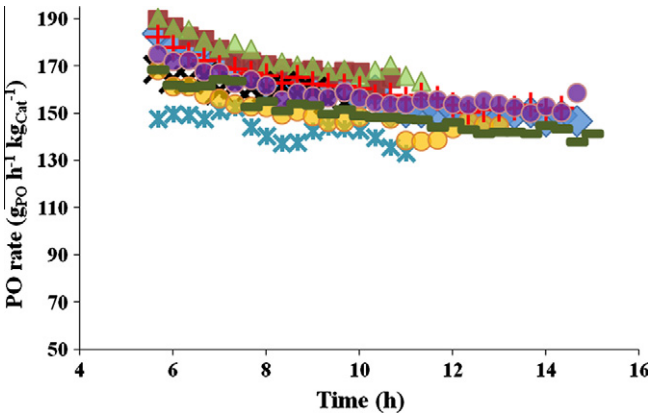

Fig. 9. Reproducibility of the rates for Au/TS-1(100) and Au/TS-1(99) catalysts prepared at pH ~ 7.3 and with a mixing time of ~9.5 h. The average PO rate was 158 g_{PO} h^{-1} kg_{Cat}^{-1} with a standard deviation of 9 g_{PO} h^{-1} kg_{Cat}^{-1}.

The gold loading is strongly affected by the pH of the slurry solution such that higher pH results in lower gold loading, as shown in Fig. 4a. A similar phenomenon was observed by the group of Oyama and coworkers, and they attribute this to a simple electrostatic model [1]. Because of the low isoelectric point of TS-1 (~2–3), a higher pH environment will establish a stronger repulsion force between the more negatively charged surface of the TS-1 and the anionic gold species. The gold loading vs. pH relationship we have found here is different from our previously published results [19]. The difference can be attributed to the use of the TS-1 with lower Si/Ti molar ratio, the lower amount of washing solution (6—18 mL g_{Cat}^{-1} instead of 25 mL g_{Cat}^{-1}), and/or the details of the washing step in the previous work, in which the catalysts were not re-suspended into 50 mL D.I. water in a flask and not stirred thoroughly for 1–2 min during washing. Although the electrostatic force explanation is consistent with the observed relation between pH and gold loading, the real gold deposition mechanism is likely to be more complex than the electrostatic attraction alone because a noticeable amount of gold can still be deposited at the very high pH of ~9. While the pH may well dominate the difficulty of the gold species to approach the TS-1 surface, the actual gold deposition could be due to a surface reaction between the gold species and the hydroxyl groups on the defect or other sites on the TS-1 surface, which is similar to the explanation proposed by Moreau et al. [26]. The defect sites in TS-1 have also been suggested via DFT calculations [32] to be energetically favorable for deposition of gold species. Recently, Dustin et al. suggested that silicalite-1 (S-1) would exhibit more defect sites if TEOS was used as the silica source [33]. Our use of S-1 as the support for normal gold deposition was also successful and the gold uptake efficiency is shown in Fig. 10a. This result suggests that even without the Ti sites serving as the preferential sites to anchor gold, some energetically favorable sites (probably defects sites) are still available for gold deposition.

Our previous experimental results, together with published DFT calculations, suggest that gold clusters smaller than 2 nm could be

Table 2
The gold loading and the catalytic performance of Au/TS-1(99) prepared at different temperatures.

Sample ID	pH	Mixing time (h)	Temp (°C)	Gold loading (wt%)	PO rate (g_{PO} h^{-1} kg_{Cat}^{-1})	Gold atom efficiency (g_{PO} h^{-1} g_{Au}^{-1})	H_2 sel. (%)
0.122Au/TS-1(99)	7.5	2	70	0.122	84	69	9.1
0.143Au/TS-1(99)	7.4	16	RT	0.143	148	103	12.1
0.146Au/TS-1(99)	7.5	16	RT	0.146	154	105	10.7

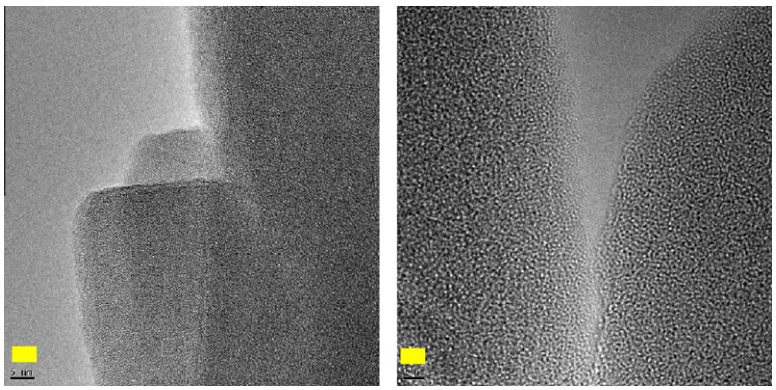

Fig. 8. TEM analysis of the fresh 0.1Au/TS-1(100) prepared at room temperature with a mixing time of 9.5 h. The scale bar represents 5 nm.

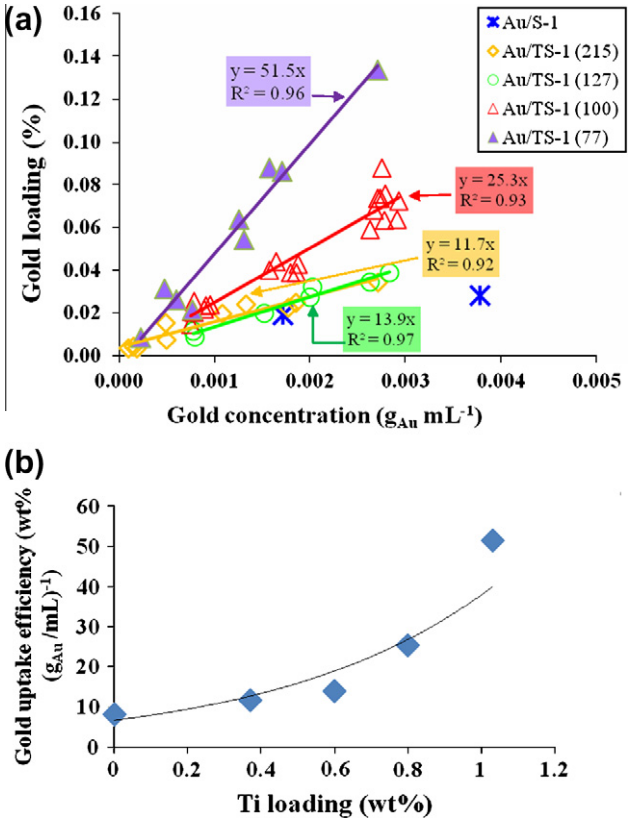

Fig. 10. (a) Gold loadings for Au/TS-1 samples with different Ti contents as a function of the concentration of gold precursor ($HAuCl_4{\cdot}3H_2O$) used in the catalyst preparation. (b) Gold uptake efficiency as a function of Si/Ti molar ratio.

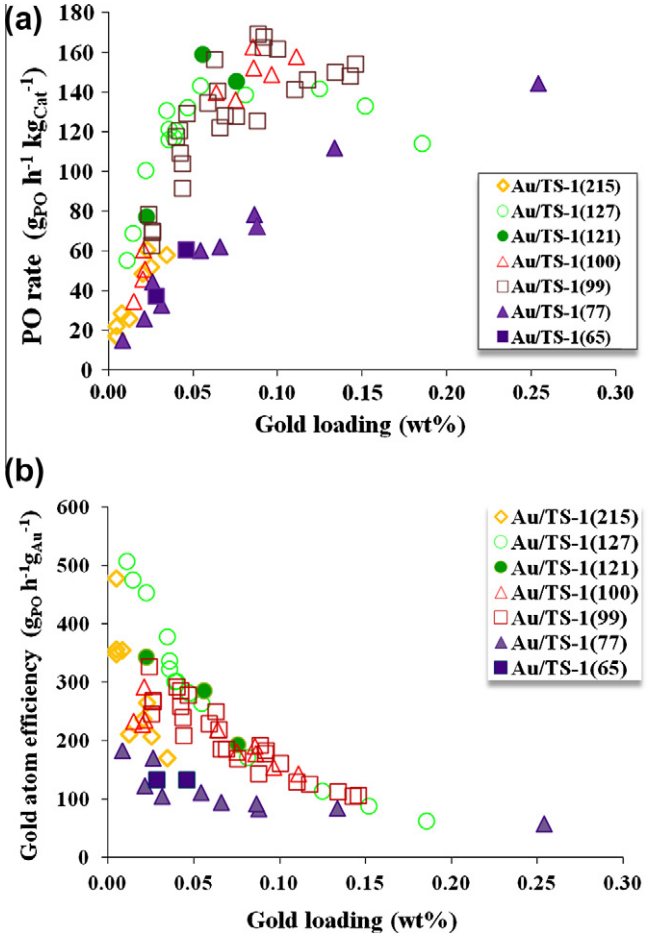

Fig. 11. (a) PO rate of the Au/TS-1 catalysts with different gold loadings prepared at pH = ~7.3. The rates are reported as average values between 3rd and 5th h. (b) Gold atom efficiency for the Au/TS-1 catalysts in 11 (a). Reaction conditions: $H_2/C_3H_6/O_2/N_2$ = 3.5/3.5/3.5/24.5 mL min^{-1}, space velocity 14,000 mL h^{-1} g_{cat}^{-1}, reaction temperature = 200 °C.

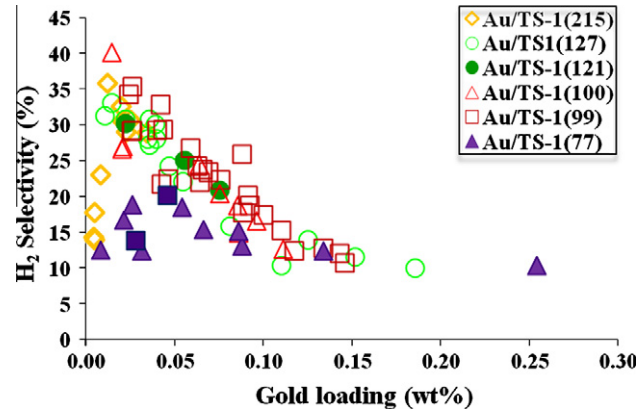

Fig. 12. H_2 selectivity of the Au/TS-1 with different gold loadings and different Si/Ti molar ratios. Reaction conditions: $H_2/C_3H_6/O_2/N_2$ = 3.5/3.5/3.5/24.5 mL min^{-1}, space velocity 14,000 mL h^{-1} g_{cat}^{-1}, reaction temperature = 200 °C. The data are reported as average values between 3rd and 5th h.

the active sites for PO reaction [17,19,32,34,35]. Recent literature shows that 1–2 nm gold clusters with a tight size distribution could be deposited on the external surface of the TS-1 by a solid grinding (SG) method [13]. The group of Haruta and coworkers suggested that the dominant active sites for PO are gold clusters with 1–2 nm diameter on the TS-1 external surface, based on the observation that samples with higher PO rate (g_{PO} h^{-1} kg_{Cat}^{-1}) exhibited higher 1–2 nm gold cluster density in the HAADF-STEM images. The gold clusters small enough to be inside the TS-1 were assigned lower activity. All these results suggest that the active gold particles should be very small regardless of whether they are inside or outside the TS-1 crystallites. A strategy for preparing Au/TS1 with high PO rate is therefore to make the gold species nearly atomically dispersed on TS-1, and then to adjust the gold cluster size further by properly choosing the activation protocol and/or reaction temperature.

Fig. 11a shows that the PO rate (g_{PO} h^{-1} kg_{Cat}^{-1}) approximately scales with the gold loading up to around 0.07 wt% for Au/TS-1(100) when the more gentle preparation condition (i.e., room temperature) was chosen for gold deposition. This linear relationship between gold loading and the PO rate performance (g_{PO} h^{-1} kg_{Cat}^{-1}) suggests that the number of active sites is also increased as the gold loading increases and implies that the gold deposition process is under control and the gold species are highly dispersed when the gold loading is below 0.07 wt%. Room temperature was chosen for gold deposition to avoid gold species aggregation because it has been reported that high preparation temperature promotes the aggregation of the gold species ($Au(OH)_xCl_{4-x}$) via the condensation reaction among the hydroxyl groups [36]. Furthermore, the gold loading was found to track with the Ti loading in Au/TS-1 system, suggesting that gold preferentially deposits over Ti sites [17]. Another potential disadvantage of higher preparation temperature is that it could over-promote the gold cluster growth at Ti sites, blocking them from participating in the epoxidation reaction. The fact that no visible gold particles could be found in the fresh Au/TS-1 with gold loading less than 0.1 wt%,

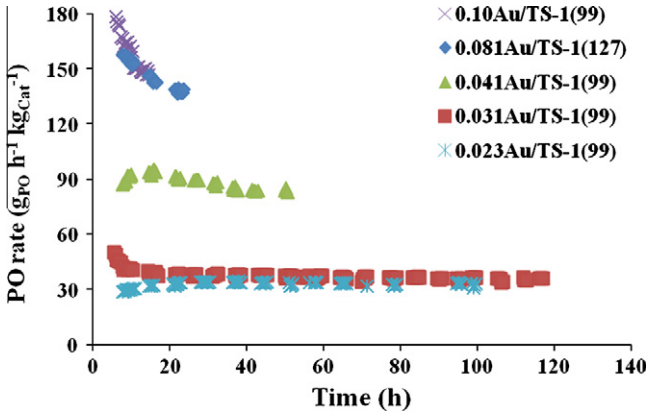

Fig. 13. Stability of Au/TS-1 samples with different PO rates. Reaction conditions: $H_2/C_3H_6/O_2/N_2$ = 3.5/3.5/3.5/24.5 mL min^{-1}, space velocity 14,000 mL h^{-1} kg_{Cat}^{-1}, reaction temperature = 200 °C. Data concerning the selectivities of the H_2 and the oxygenated products (PO, ethanal (Et), propanal (Pr), acetone (Ac), and acrolein (An)), the propylene conversion, and the production rate of the oxygenates other than PO as a function of the reaction time are available in the supporting information (Figs. S12–21).

as shown in Fig. 8, supports the conclusion that gold species can be deposited in a very high dispersion from room temperature preparation. Fresh samples prepared by using the 70 °C, 2 h conventional preparation conditions with similar gold loading (~0.1 wt%) showed visible gold particles with average size ~2 nm in the literature [1] and, as shown in Table 2, lower gold atom efficiency compared to room temperature preparation.

The linear relationship between the gold loading and the PO rate shown in Fig. 11a provides the motivation to seek ways to expand the plot to higher rates. Increasing loading by raising the temperature has already been shown to be unsuccessful. We decided to increase the gold slurry mixing time as an alternative, mild way to increase loading. When the mixing time increased from 5 h to 9.5 h, the PO rate also increased from an average value of 136 to 160 g_{PO} h^{-1} kg_{Cat}^{-1} at 200 °C, as shown in Fig. 7. Considering that TS-1 is a hydrophobic material and that electrostatic force at useful pH is also not favorable, gold complex species are relatively hard to deposit on the TS-1. Thus, it is likely that the deposition processes are kinetically controlled and that the contact time between the support and the gold species can directly affect the production of the active sites for PO reaction. Longer contact time allows the gold species to diffuse into the microporous channels and increase reaction with surface hydroxyl groups and/or the defect sites. Moreover, longer mixing time also allows evolution of the slow room temperature hydrolysis reactions between the chloride and the hydroxyl ion in solution so that most of the undesired chloride ligands, which are known to be detrimental for CO oxidation, would be replaced by hydroxyl groups. It should be noted that this level of control in the gold atom efficiency for the PO reaction (g_{PO} h^{-1} g_{Au}^{-1}) at this wide gold loading range is unprecedented in the literature. We concluded that the essential keys to preparing the Au/TS-1 with PO rate over 100 g_{PO} h^{-1} kg_{Cat}^{-1} are to choose room temperature together with the longer mixing time as the more gentle preparation conditions, instead of the commonly used high preparation temperature (50–80 °C) with shorter preparation time. It is interesting to note that the linear response of the rate to gold loading found here also provides confirmation, by the Koros–Nowak/Madon–Boudart criterion [37,38] that the rates are not transport controlled.

Two special features of TS-1, low isoelectric point and a hydrophobic surface, make it inappropriate to apply the deposition–precipitation (DP) method for gold deposition. However, it appears that the deposition inefficiency caused by these two features is what leads to gold species that still remain highly dispersed in Au/TS-1 even when very high concentration of the gold precursor solution (nominal gold loading ~5.5 wt%) is used for gold catalyst preparation. The idea that high activity of the Au/TS-1 can be achieved by using properly chosen DP conditions (using nominal gold solution loading as high as ~10 wt% and synthesizing at room temperature) has also been supported by the recent report by Mennemann and Claus [39] in which the Au/TS-1 with gold loading ~0.05 wt% and Si/Ti molar ratio ~46 showed a PO rate ~68 g_{PO} h^{-1} kg_{Cat}^{-1}, comparable to the PO rate ~60 g_{PO} h^{-1} kg_{Cat}^{-1} of the 0.054Au/TS-1(77) catalyst prepared in this work.

Based on the experimental data reported in this work, no further information could be provided regarding the assignment of active sites to gold clusters inside and/or outside the TS-1 crystallites, although the decrease in gold atom efficiency as the gold loading increases indicates that the active gold cluster size should be small. In Fig. 14, the HRTEM image of the 0.1Au/TS-1(99) after ~14 h of reaction showed an average gold particle size around ~2.9 nm, while that of the 0.03Au/TS-1(99) after ~116 h in reaction was around ~2.5 nm. If we consider that (1) the gold loading of the 0.1Au/TS-1(99) was three times that of 0.03Au/TS-1(99), (2) the total visible gold particle density (#/ nm^2, calculated from the TEM images in which gold particles could be observed) of 0.1Au/TS-1 was only ~40% of that for 0.03Au/TS-1(99), (3) most of the gold in 0.03Au/TS-1(99) could have already moved toward the surface because of the long exposure time (>100 h) at the reaction temperature 200 °C, and (4) the 0.1Au/TS-1(99) has a rate >4 times that of 0.03Au/TS-1(99), we can conclude that gold clusters "invisible" by HRTEM in 0.1Au/TS-1 could contribute significant activity for the PO reaction. Finally, the highest gold atom efficiency yet reported (500 g_{PO} h^{-1} g_{Au}^{-1}) is for a sample with very low gold loading, 0.01Au/TS-1(127), supporting the conclusion that gold clusters smaller than 2 nm are very active for the PO reaction [13].

4.2. Effects of Si/Ti molar ratio on PO rate

The natural intuition for enhancing the PO rate (g_{PO} h^{-1} kg_{Cat}^{-1}) further still is to provide as many Ti sites as possible in the TS-1. This idea leads to the use of Ti containing supports with lower Si/Ti molar ratio for preparing Au/titanosilicalite catalysts for PO reaction [8–11,40]. Previous studies of the effect of the Si/Ti molar ratio on the PO catalytic performance showed that the gold atom efficiency was inferior for samples with higher Ti content [1,17], but changes in Au loading at different Si/Ti molar ratios complicate interpretation. In an effort to better understand the effect of the Ti content on the PO catalytic performance, we used the concentration of gold precursor and/or the mixing time to control the Au loading and prepared samples with different gold loadings for several Si/Ti molar ratios using a pH of ~7.3 and room temperature. It was found unexpectedly that the gold atom efficiency was always much lower for the Au/TS-1 with higher Ti contents (Si/Ti = 77 and/or 65), compared to the ones with lower Ti contents (Si/Ti = 127, 121 and/or 99, 100). Moreover, in the gold loading range investigated, the best performance in the PO rate was found for TS-1 supports with Si/Ti ~ 100. This suggests that the optimum window for the Si/Ti molar ratio for Au/titanosilicalite catalysts prepared by the DP method for the PO reaction should be shifted to around 100, instead of the widely used Si/Ti molar ratio values of 30–100 found in the literature [8–11,40].

The exact reason for this phenomenon is unclear. The effect of the total or external surface area of the support on the PO catalytic performance can be excluded because, as shown in Table 1, the variations are small. Furthermore, Table 1 shows that the spatial distribution of the Ti in both TS-1(100) and TS-1(77) was uniform since the surface Si/Ti and the bulk Si/Ti molar ratios were similar. Even though no peaks/shoulders around 260 nm were observed in the UV–vis spectra for all the TS-1 investigated in this work, it is

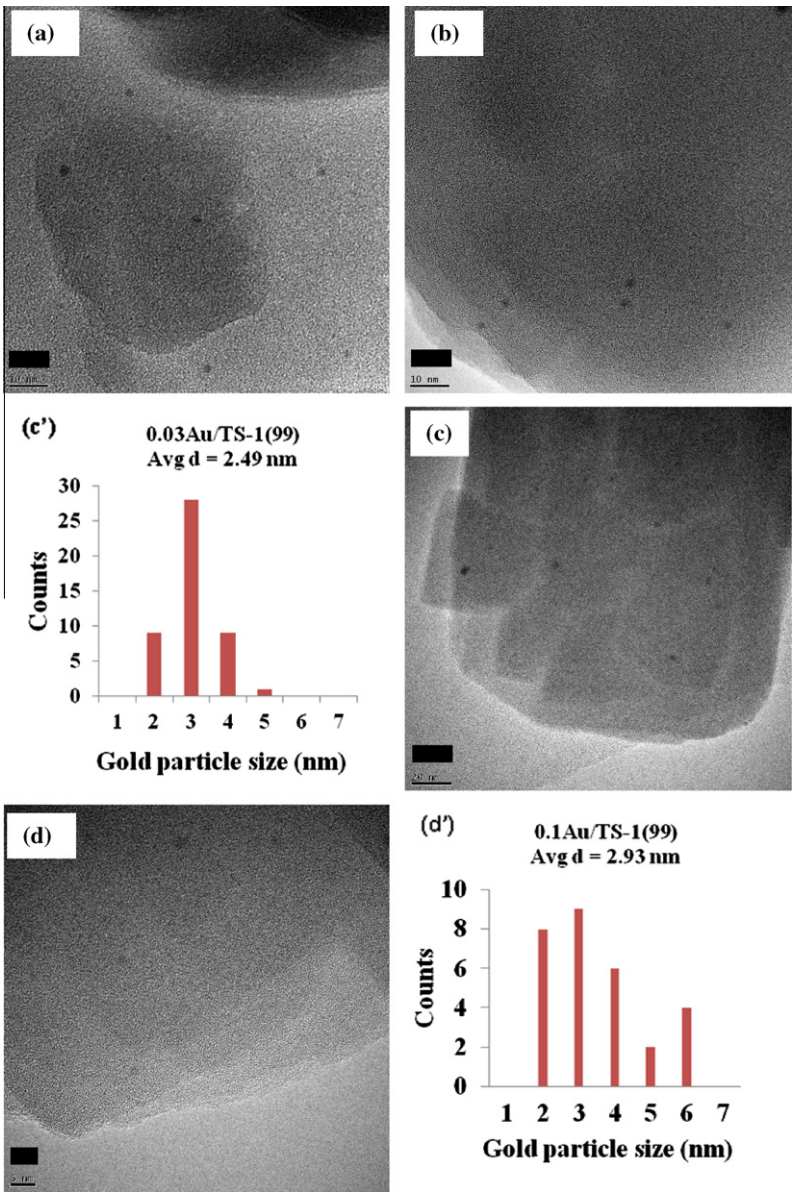

Fig. 14. (a–c) TEM images and (c') particle size distributions for spent 0.03Au/TS-1(99) with PO rate ~35 g_{PO} h^{-1} kg_{Cat}^{-1} after ~116 h reaction at 200 °C. The scale bar represents 10 nm in (a-b) and 20 nm in (c). (d) TEM images and (d') particle size distributions for spent 0.1Au/TS-1(99) with PO rate ~150 g_{PO} h^{-1} kg_{Cat}^{-1} after 14 h reaction. The scale bar represents 5 nm.

still possible that a very small amount of the extraframework Ti might be present in TS-1 with higher Ti content [41]. To examine this possibility further, we turned to the PO and H_2 selectivity. With the current experimental setup, the precise measurement of the PO selectivity is not available since the use of nitrogen as the carrier gas results in a weak TCD signal for CO_2. Nevertheless, the PO selectivity (even without considering the CO_2) can still be a good indicator of the effect of the support on the PO performance. Fig. 15 shows that the PO selectivity of Au/TS-1 with higher Ti contents (Si/Ti = 77 and 65) is much lower than that of Au/TS-1 with lower Ti contents (Si/Ti = 127, 121 and 99, 100). The loss of the PO selectivity in the Au/TS-1 with Si/Ti = 77 and/or 65 was driven by an increase of the propanal selectivity (not shown). This change in the partial oxidation product distribution as well as the lower hydrogen peroxide usage efficiency (lower H_2 selectivity) suggests the presence of some extraframework Ti, since it was found that the PO selectivity and the other oxygenate product distribution can be a strong function of the Ti–O–Ti connectivity [6], and the extraframework Ti is known as a good catalyst for hydrogen peroxide decomposition [42]. This also implies the importance as well as the sensitivity of the PO catalytic performance on the Ti coordination state.

4.3. Effects of Si/Ti molar ratio on H_2 selectivity

As for the H_2 selectivity, Au/TS-1 with lower Ti content (Si/Ti $\geqslant$ 99) generally showed increased H_2 selectivity as the gold loading decreased. It has been reported that larger gold particles (~2 nm) promote H_2 combustion in an Au/mesoporous titanosilicalite system [8]. The decreased H_2 selectivity at higher gold loading might be due, therefore, to the presence of the larger gold particles. The effect of gold particle size on H_2 combustion will be discussed in a later paper, but the exact reason why (1) the H_2 selectivity for the Au/TS-1(77) is essentially independent of the gold loading from ~0.03 wt% to ~0.13 wt% and (2) the H_2 selectivity for the Au/TS-1(215) started to drop when the gold loading less than 0.01 wt% remains unclear.

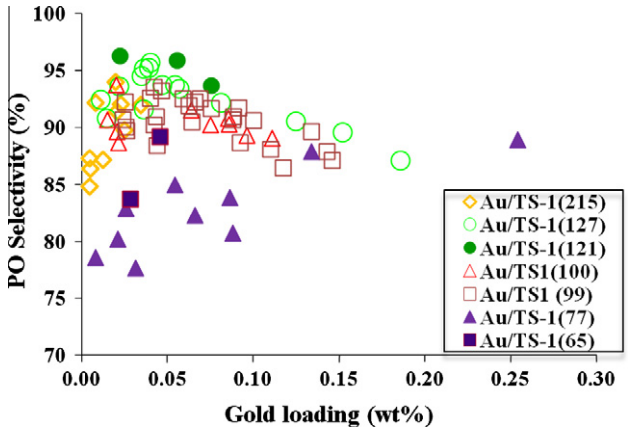

Fig. 15. PO selectivity of Au/TS-1 catalysts with different gold loadings and different Si/Ti molar ratios. The data are reported as the average values between 3rd and 5th h at 200 °C. Reaction conditions: $H_2/C_3H_6/O_2/N_2$ = 3.5/3.5/3.5/24.5 mL min^{-1}, space velocity 14,000 mL h^{-1} g_{cat}^{-1}, reaction temperature = 200 °C.

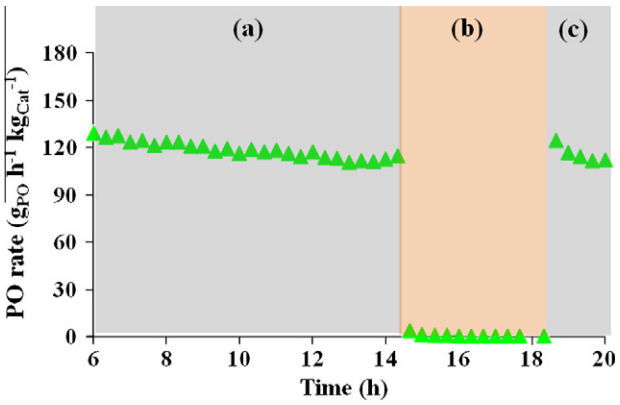

Fig. 17. Regeneration test for 0.04Au/TS-1(127) during PO reaction. (a) catalyst at reaction conditions, (b) catalyst in O_2/N_2 = 3.5/24.5 mL min^{-1} at 200 °C for ~4 h, and (c) catalyst switched back to reaction conditions. Reaction conditions: $H_2/C_3H_6/O_2/N_2$ = 3.5/3.5/3.5/24.5 mL min^{-1}, space velocity 14,000 mL h^{-1} g_{cat}^{-1}, reaction temperature = 200 °C.

Another interesting issue is whether or not the physical features and/or chemical properties of the TS-1 remain the same when the Ti content varies. Defect sites in TS-1 are relevant because they have been shown to be energetically favorable for gold deposition and/or PO reaction as described above. Previous study of the sorption properties of calcined TS-1 with different Ti contents showed that the water sorption capacity increases as the Si/Ti ratios decrease from 99 to 48. This measure of hydrophylicity indicates that either the number of defect sites is higher or the water has stronger affinity toward Ti sites for the TS-1 with higher Ti content [43,44]. Our thermogravimetric analysis (TGA) data, shown in Fig. 16, suggest that our TS-1 with higher Ti content was also more hydrophilic (more water loss at 250 °C). As discussed above, the gold loading increased as the Si/Ti molar ratio decreased, but the gold uptake efficiency was a nonlinear function of the Ti content. The nonlinear increase in the gold loading as the Ti content increases could be caused by the number of the defect sties (including both Si defect sites and Ti defect sites) being a nonlinear function of the Ti content in our TS-1 coupled with a nonlinear interaction of Au with these sites. Additionally, the new defect sites (including both Si defect sites and Ti defect sites) might be generated during the gold deposition process. The finite gold uptake in S-1 and the nonlinear dependence between the gold uptake and the Ti content in the TS-1 suggest the defect sites play an important role in the gold deposition process for Au/TS-1. Therefore, the distribution of the gold species between the Si defect sites and the Ti sites might be a function of the gold loading and/or the Si/Ti molar ratio, which would affect the number of PO active sites (Au–Ti proximity sites), the gold cluster size as well as the extent of gold particle sintering at the given gold loading. The imbalanced distribution of the deposited gold species toward the Si defect sites and Ti sites on the TS-1 might also contribute to the unexpected H_2 selectivity behavior in Au/TS-1(215) and/or Au/TS-1(77) at different gold loadings.

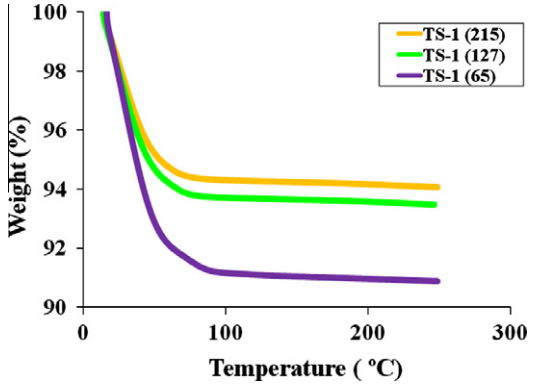

Fig. 16. TGA analysis for TS-1 catalysts with different Ti contents. The samples (~20–40 mg) were not sieved prior TGA analysis. The temperature was raised from room temperature to 250 °C at a ramping rate 5 °C min^{-1} in a flow of He of ~100 mL min^{-1}.

4.4. Catalyst stability

Finally, we consider catalyst stability. We attribute the significant PO activity loss of the samples with initial PO rate > 100 g_{PO} h^{-1} kg_{Cat}^{-1} to gold particle aggregation during the stability test at 200 °C. When the gold loading is lower, however, the distance between the gold particles becomes larger, which reduces the probability of gold cluster/particle sintering, and the catalysts showed very good stability even over 100 h. In addition to the gold particle sintering, bidentate species that form during the reaction on the surface [5] and can block the active site have been suggested to the reason for the catalyst deactivation [1,5]. The bidentate species, together with other species (acetates), has also been found to track with catalyst (Au–Ba/Ti-TUD) deactivation in an in situ IR experiment [45]. However, the question of whether or not the rate of the bidentate species building up correlates with the deactivation rate in the Au/TS-1 system remains unanswered. An attempt to restore the PO rate by switching the reaction mixture to O_2/N_2 = 3.5/24.5 mL min^{-1} at 200 °C for ~4 h to burn off the residual carbon on the catalyst surface seems to have been successful (shown in Fig. 17), as the PO rate after regeneration (124 g_{PO} h^{-1} kg_{Cat}^{-1}) is comparable to that of the fresh sample (130 g_{PO} h^{-1} kg_{Cat}^{-1}). However, the catalyst continued to decay for the following 1–2 h of reaction. We note that by performing an *operando* IR experiment, one could clearly address the effect of the surface adsorbates on catalyst deactivation. The different catalytic behavior modes of the two catalysts, 0.031Au/TS-1(99) and 0.023Au/TS-1(99), imply that the dynamics of the gold species during the reaction are different and may be correlated to the different pHs used in the preparation conditions.

5. Conclusions

By optimizing the preparation conditions (the pH of the gold slurry solution, the mixing time, and the preparation temperature),

a PO rate ~160 $g_{PO}\ h^{-1}\ kg_{Cat}^{-1}$ was achieved, which is the highest PO rate at 200 °C yet reported. Good control of Au/TS-1 preparation was demonstrated by the reproducibility of nine individual samples. Very high gold atom efficiency (~500 $g_{PO}\ h^{-1}\ g_{Au}^{-1}$) was found for Si/Ti~127 samples with gold loading as low as ~0.01 wt%, suggesting that the smallest gold clusters are the most active for the PO reaction. Additionally, the gold atom efficiency was found to be a function of the Si/Ti mole ratio of the TS-1. Instead of TS-1 with high Ti content to increase the site density, diluted systems (low gold loading/low Ti loading) are recommended for preparing Au/TS-1 with high reaction rate for PO production. The stability of the samples with different gold loadings and PO rates suggests that the PO rate is very sensitive to the gold cluster size, with sparsely loaded clusters <2 nm being the most stable as well as the most active. Stability over 100 h on stream was demonstrated for a sample with PO rate ~35 $g_{PO}\ h^{-1}\ kg_{Cat}^{-1}$, while a more active sample with PO rate $> 100\ g_{PO}\ h^{-1}\ kg_{Cat}^{-1}$ still suffered from deactivation, which we propose is caused by the loss of the optimally active gold cluster size.

Acknowledgments

Support from the Department of Energy, Office of Basic Energy Sciences, Chemical Sciences, under Grant DE-FG02-03ER15408 is gratefully acknowledged. Electron microscopy carried out in part at the Center for Functional Nanomaterials, Brookhaven National Laboratory, which is supported by the U.S. Department of Energy, Office of Basic Energy Sciences, under Contract No. DE-AC02-98CH10886.

Appendix A. Supplementary material

Supplementary data associated with this article can be found, in the online version, at doi:10.1016/j.jcat.2011.12.019.

References

[1] J.Q. Lu, X.M. Zhang, J.J. Bravo-Suarez, T. Fujitani, S.T. Oyama, Catal. Today 147 (2009) 186–195.
[2] T.A. Nijhuis, M. Makkee, J.A. Moulijn, B.M. Weckhuysen, Ind. Eng. Chem. Res. 45 (2006) 3447–3459.
[3] M. Haruta, B.S. Uphade, S. Tsubota, A. Miyamoto, Res. Chem. Intermed. 24 (1998) 329–336.
[4] T. Hayashi, K. Tanaka, M. Haruta, J. Catal. 178 (1998) 566–575.
[5] G. Mul, A. Zwijnenburg, B. van der Linden, M. Makkee, J.A. Moulijn, J. Catal. 201 (2001) 128–137.
[6] E.E. Stangland, B. Taylor, R.P. Andres, W.N. Delgass, J. Phys. Chem. B 109 (2005) 2321–2330.
[7] J.J. Bravo-Suarez, J. Lu, C.G. Dallos, T. Fujitani, S.T. Oyama, J. Phys. Chem. C 111 (2007) 17427–17436.
[8] J.Q. Lu, X.M. Zhang, J.J. Bravo-Suarez, K.K. Bando, T. Fujitani, S.T. Oyama, J. Catal. 250 (2007) 350–359.
[9] A.K. Sinha, S. Seelan, M. Okumura, T. Akita, S. Tsubota, M. Haruta, J. Phys. Chem. B 109 (2005) 3956–3965.
[10] B.S. Uphade, T. Akita, T. Nakamura, M. Haruta, J. Catal. 209 (2002) 331–340.
[11] B.S. Uphade, Y. Yamada, T. Akita, T. Nakamura, M. Haruta, Appl. Catal., A 215 (2001) 137–148.
[12] L. Cumaranatunge, W.N. Delgass, J. Catal. 232 (2005) 38–42.
[13] J.H. Huang, T. Takei, T. Akita, H. Ohashi, M. Haruta, Appl. Catal., B 95 (2011) 430–438.
[14] T. Liu, P. Hacarlioglu, S.T. Oyama, M.F. Luo, X.R. Pan, J.Q. Lu, J. Catal. 267 (2009) 202–206.
[15] E.E. Stangland, K.B. Stavens, R.P. Andres, W.N. Delgass, J. Catal. 191 (2000) 332–347.
[16] B. Taylor, J. Lauterbach, G.E. Blau, W.N. Delgass, J. Catal. 242 (2006) 142–152.
[17] B. Taylor, J. Lauterbach, W.N. Delgass, Appl. Catal., A 291 (2005) 188–198.
[18] B. Taylor, J. Lauterbach, W.N. Delgass, Catal. Today 123 (2007) 50–58.
[19] N. Yap, R.P. Andres, W.N. Delgass, J. Catal. 226 (2004) 156–170.
[20] T.A. Nijhuis, B.J. Huizinga, M. Makkee, J.A. Moulijn, Ind. Eng. Chem. Res. 38 (1999) 884–891.
[21] M. Du, G. Zhan, X. Yang, H. Wang, W. Lin, Y. Zhou, J. Zhu, L. Lin, J. Huang, D. Sun, L. Jia, Q. Li, J. Catal. 283 (2011) 192–201.
[22] M.C. Kung, R.J. Davis, H.H. Kung, J. Phys. Chem. C 111 (2007) 11767–11775.
[23] M. Haruta, Catal. Today 36 (1997) 153–166.
[24] M. Haruta, J. New Mat. Electrochem. Syst. 7 (2004) 163–172.
[25] J.N. Lin, B.Z. Wan, Appl. Catal., B 41 (2003) 83–95.
[26] F. Moreau, G.C. Bond, A.O. Taylor, J. Catal. 231 (2005) 105–114.
[27] R.B. Khomane, B.D. Kulkarni, A. Paraskar, S.R. Sainkar, Mater. Chem. Phys. 76 (2002) 99–103.
[28] J. Gaudet, K.K. Bando, Z.X. Song, T. Fujitani, W. Zhang, D.S. Su, S.T. Oyama, J. Catal. 280 (2011) 40–49.
[29] W.-S. Lee, R. Zhang, M.C. Akatay, C.D. Baertsch, E.A. Stach, F.H. Ribeiro, W.N. Delgass, ACS Catal. 1 (2011) 1327.
[30] G.N. Vayssilov, Catal. Rev. Sci. Eng. 39 (1997) 209–251.
[31] R. Millini, E.P. Massara, G. Perego, G. Bellussi, J. Catal. 137 (1992) 497–503.
[32] A.M. Joshi, W.N. Delgass, K.T. Thomson, J. Phys. Chem. C 111 (2007) 7841–7844.
[33] D.W. Fickel, A.M. Shough, D.J. Doren, R.F. Lobo, Micropor. Mesopor. Mater. 129 (2010) 156–163.
[34] A.M. Joshi, W.N. Delgass, K.T. Thomson, J. Phys. Chem. B 109 (2005) 22392–22406.
[35] A.M. Joshi, W.N. Delgass, K.T. Thomson, J. Phys. Chem. B 110 (2006) 2572–2581.
[36] S. Ivanova, V. Pitchon, C. Petit, H. Herschbach, A. Van Dorsselaer, E. Leize, Appl. Catal., A 298 (2006) 203–210.
[37] R.M. Koros, E.J. Nowak, Chem. Eng. Sci. 22 (1967) 470.
[38] R.J. Madon, M. Boudart, Ind. Eng. Chem. Fund. 21 (1982) 438–447.
[39] C. Mennemann, P. Claus, Catal. Lett. 134 (2010) 31–36.
[40] C.X. Qi, T. Akita, M. Okumura, K. Kuraoka, M. Haruta, Appl. Catal., A 253 (2003) 75–89.
[41] A. Tuel, L.G. Hubert-Pfalzgraf, J. Catal. 217 (2003) 343–353.
[42] D.R.C. Huybrechts, P.L. Buskens, P.A. Jacobs, J. Mol. Catal. 71 (1992) 129–147.
[43] S.P. Mirajkar, A. Thangaraj, V.P. Shiralkar, J. Phys. Chem. 96 (1992) 3073–3079.
[44] L.Y. Chen, G.K. Chuah, S. Jaenicke, J. Mol. Catal. A: Chem. 132 (1998) 281–292.
[45] J.J. Bravo-Suarez, K.K. Bando, J.I. Lu, M. Haruta, T. Fujitani, S.T. Oyama, J. Phys. Chem. C 112 (2008) 1115–1123.